

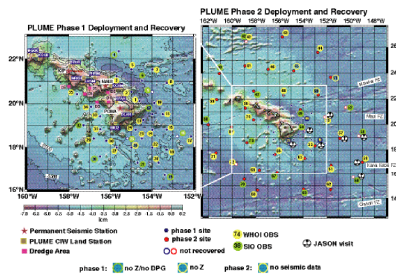


The Hawaiian PLUME deployment: Lessons learned and recommendations for a Galapagos deployment

Gabi Laske, IGPP, Scripps Institution of Oceanography, UCSD

The Hawaiian PLUME Experiment

The interdisciplinary PLUME-Lithosphere Undersea Meft Experiment (PLUME) studies the shape and origin of the mantle plume beneath the Hawaiian hotspot. The centerpiece of this 5-year project is an unprecedented long-term deployment of broad-band OBSs (ocean bottom seismometers) to record local and teleseismic earthquakes.

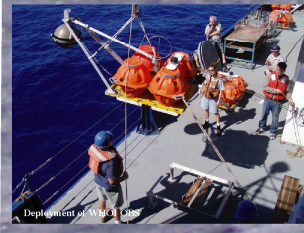
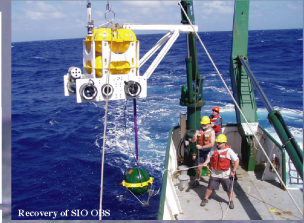
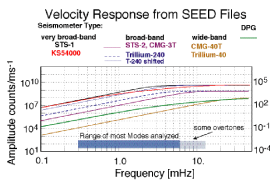


Deployment Logistics
 * January 2005 - January 2006: PLUME 1
 * April 2006 - May 2007: PLUME 2
 * Nov. 2007: JASON rescue attempt at 8 OBS sites

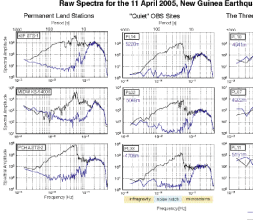
The PLUME network consisted of a 2-phase deployment of broadband OBSs plus 10 land stations. Phase 1 was placed above the proposed location of the plume conduit for fine-scale imaging. Phase 2 was intended for a well-covering surface wave study as well as to give the body-wave study greater depth-sensitivity.

Seismic Sensors

SENSORS:
 Land Stations: Wieland-Streckeisen STS-2: 20 Hz
 WHOI OBSs: Curalp CMA-3T: 1, 20 Hz (DPG 40 Hz)
 SIO OBSs: PLUME1: Nanometrics Trillium 40: 31, 25 Hz
 SIO OBSs PLUME2: Nanometrics Trillium 240: 31, 25 Hz
 Permanent KIP: STS-1
 Permanent NOAA: Geotech Trillium KSS4000
 GEOPON MAUI: STS-2
 OBSs: Cox-Webb differential pressure gauge (DPG)

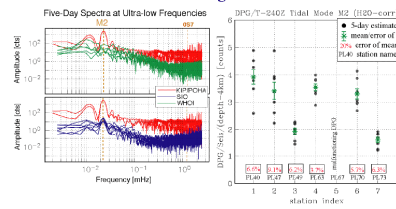


Broadband Signal-to-Noise Levels



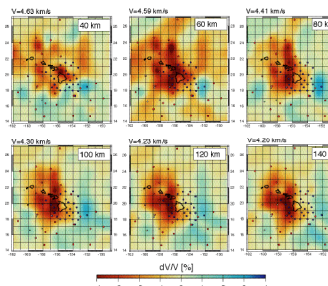
Vertical-component spectra of 20-min-long segments before and during an earthquake. A large gap between the spectra signifies a high signal-to-noise ratio, hence a "quiet" station, for the purposes of earthquake seismology, this approach is more revealing than assembling the standard ambient noise plots. The water depth at each OBS station is given below its name. Colored bars beneath the middle panel mark the two noise bands, the microseism band above 0.05 Hz as well as the infragravity band below 0.01 Hz. The range in between is known as the noise notch.

In-Situ DPG Calibration Using Tides



LEFT: The vertical components of the SIO seismometers (Nanometrics Trillium-240) have a noise level low enough to observe tidal modes. **MIDDLE:** Surprisingly, the SIO DPGs also show tidal signals with a very high signal-to-noise ratio. The fact that an unintended instrument-generated harmonic signal on the seismometer is not visible on the DPG confirms that the tidal signal on the DPG comes from the sensor itself and not through electronic cross-coupling with the seismometer. **RIGHT:** An attempt to calibrate the DPGs in situ by comparing the M2 amplitudes with those on the seismometer. A signal dependent on water depth was removed. The attempt confirms that DPG amplitudes can vary by a factor 2, but with just 5 days of data, we are able to determine calibration factors to better than 10%. A more accurate re-calibration using longer records is underway.

Vs Model of Lithosphere and Asthenosphere from Rayleigh Wave Tomography



LEFT: The 2-station method was used to determine path-averaged phase velocity curves along 614 paths. These curves were used to construct maps of local phase velocity, at fixed frequency. Finally, these maps were used as "data" in a tomographic inversion for 3-D shear velocity structure. Shown are percentage velocity perturbations to the reference model (modified Nishimura and Foreth, 1989 model for 100 Ma old oceanic lithosphere).

Vs Model of Upper and Lower Mantle from S Wave Tomography

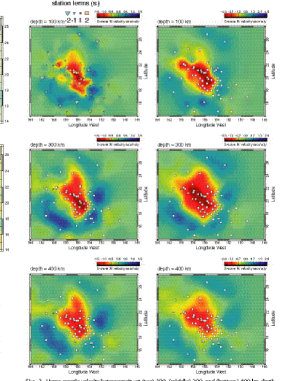
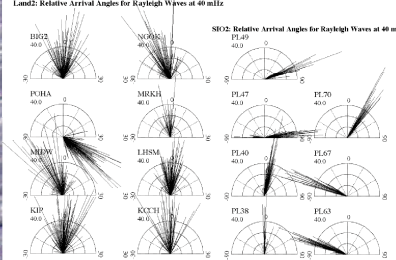


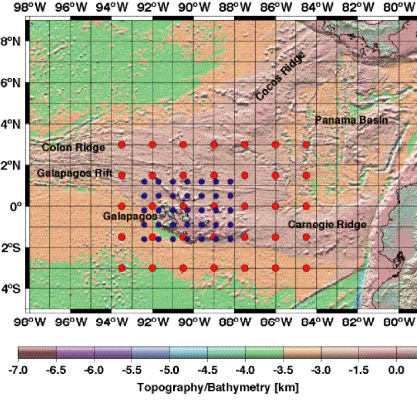
Fig. 3: Upper mantle velocity heterogeneity at 100, 150, 200, 300, and 400 km depth. The scale of heterogeneity is indicated in the color at the center of each panel. The left column (bottom station) shows the heterogeneity with station names. The right column shows the heterogeneity at an oceanic reference station name.

A-Posteriori Alignment of Horizontal Components



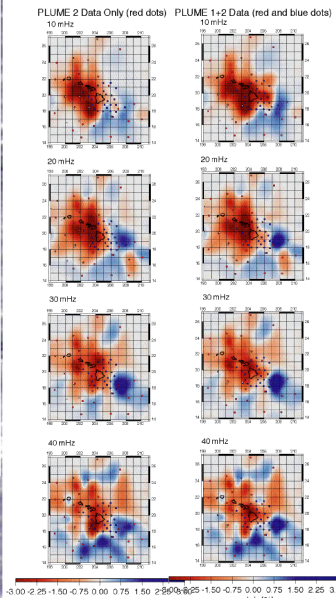
We determine the orientation of the horizontal seismometer components during post-processing. For each surface wave packet, we determine the dominant azimuth of the particle motion using the method of Laske and Masters (1995, 1996) (decomposition of the frequency-dependent 3-component spectral density matrix, for both Love and Rayleigh waves). Arrival angles are then represented as deviations with respect to the receiver-source-back azimuth, for each earthquake (shown above for land stations - left - and SIO phase-2 OBSs - right, for Rayleigh waves at 40 mHz). Arrival angles are sensitive to along-path variations in phase velocity and so cause a scatter in the observations. In a joint inversion for phase velocity maps and station misorientation, the latter is determined at several frequencies. In a least-squares sense, the weighted average is the best-fitting misalignment.

A Strawman Galapagos OBS Deployment



A possible 2-phase deployment of 35 OBSs each could cover a 600 km x 900 km area. Note though that the bathymetry is much shallower than near the Hawaiian PLUME deployment.

The Impact of Local Instrument Densification



LEFT: Phase velocity maps obtained at 4 frequencies using only data from the sparser phase-2 deployment.
RIGHT: Phase velocity maps after adding data from the denser phase-1 deployment. Small-scale features within the phase-1 array are now much better resolved than before.

OBS re-alignments are typically constrained by 90 Rayleigh wave data, at each frequency, and 45 Love wave data. Land station values typically constrained by 130 Rayleigh wave data, and 70 Love wave data. For good stations but bad stations are constrained by much less. For example, phase-2 MRKH is constrained by 45 Rayleigh wave data and 17 Love wave data. Both the number of data as well as the variance weigh in on the final error bars.